EFFECTS OF OTHER-SECTOR INTERFERENCE VARIATION ON DETECTION, LINK ADAPTATION, AND SCHEDULING IN HSDPA

Lars T. Berger
Preben E. Mogensen
Department of Communication Technology, Aalborg University
Fredrik Bajers Vej 7A
9220 Aalborg, Denmark

Troels E. Kolding
Frank Frederiksen
Klaus I. Pedersen
Nokia Networks, Aalborg R&D
Niels Jernes Vej 10
9220 Aalborg, Denmark

ABSTRACT

This paper analyses other-sector interference variation effects in the context of 3G WCDMA/HSDPA. It focuses particularly on the on/off power switching effect caused by partial HSDPA inactivity and on fast transmit antenna weight adaptation which occurs when closed loop transmit diversity is used. It is found that partial HSDPA inactivity and/or closed loop transmit diversity operation can cause symbol level SINR variation in the order of 2-4 dB. In the considered system with 56 interfering sectors, this leads to cell throughput losses up to 10% with proportional fair scheduling and perfect channel state feedback. Including channel quality indication inaccuracies, however, effects due to other-sector interference variation become negligible.

I. INTRODUCTION

Delay tolerance of packet data traffic allows the introduction of channel quality dependent *packet scheduling* (PS) to the downlink of evolving 3G packet data systems. One scheduling method which has gained particular attention is the *proportional fair* (PF) PS algorithm, which allocates radio resources to users when they are in favourable channel conditions with respect to their average situation [1]. PF PS is commonly based on explicit *channel quality indication* (CQI) feedback sent from all users to the base station (Node-B). The high performance of PF scheduling is dependent on the trackability of the radio channel conditions, i.e. it requires that there is little channel quality variation between the time of CQI estimation at the *user equipment* (UE) and the time of the actual downlink packet data transmission. In WCDMA/HSDPA, a commonly assumed delay is 6 ms [2], which is the equivalent of three *transmit time intervals* (TTIs). Variability of the channel quality – or rather of the *signal to interference plus noise ratio* (SINR) at the user's detector – has typically been attributed to Doppler effects. Among others, it has been shown in [2] that at UE velocities exceeding 20-30 km/h the performance benefit of PF PS over blind Round-Robin or *fair resource* (FR) PS is minimal. In this paper, further variability mechanisms are considered which take place independent of the UE velocity. These effects are related to changing received interference powers from other sectors as depicted in Fig. 1.

To start with, the HSDPA data channels (the *high speed downlink shared channels*, HS-DSCH) can undergo on/off pulsing of the channel transmit power if no data is available for scheduling, e.g. the system is dimensioned conservatively for high quality of service, in which case it is not running under full load but allows for some throughput headroom. If simultaneously a large fraction of the total sector transmit power is allocated to HSDPA traffic, this may lead to large instantaneous SINR variations at the UE detector as shown in Fig. 1.

Secondly, if the sectors deploy multiple transmit antenna schemes like *closed loop transmit diversity mode 1* (CLM1) [3], updating of transmit antenna weights especially when switching to a different user can cause significant and abrupt interference power variations. Moreover, the pace of variability for these two mechanisms is potentially very high; e.g. several variations may occur within a single TTI.

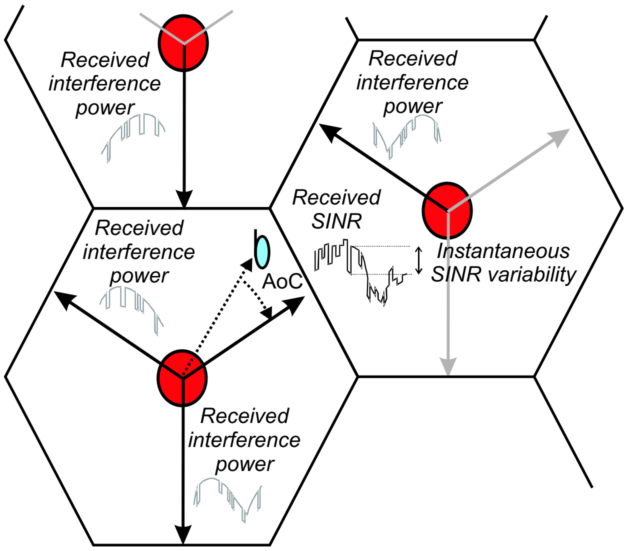

Figure 1. Impact of other-sector interference variability on SINR, where black arrows indicate accurately modelled sectors.

In this paper, the goal is to evaluate the impact of these mechanisms and to assess what is the potential degradation seen in terms of overall cell level throughput. Degradations due to rapid other sector interference variation can be threefold and these mechanisms are assessed separately in the paper: (i) Direct detector degradation caused by SINR variation within a TTI, (ii) link adaptation imperfections, and (iii) scheduling decision errors, where (ii-iii) are caused mainly by channel quality variations from the time of the channel quality estimate to the actual packet data transmission. In the following sections, some general definitions related to variability, the system set-up, the simulation strategy, and the employed assumptions are presented. This is followed by detailed simulation results and conclusions.

II. Variability Definitions

To study the impact of variability on link and system performance, the SINR experienced at the UE detector prior to decoding is used. Let the slot level SINR be defined as

$$\mathrm{SINR_{slot}}[n] = \mathrm{E_{slot}}\left\{\frac{E_s}{I_0}\right\} \quad , \qquad (1)$$

where E_s/I_0 is the instantaneous SINR of a received symbol and $E_{slot}\{\cdot\}$ represents slot-time average. Similarly, the TTI level SINR is defined as

$$\mathrm{SINR_{TTI}}[m] = \mathrm{E_{TTI}}\{\mathrm{SINR_{slot}}\} \quad , \qquad (2)$$

where one TTI comprises three consecutive slots. Using (1) a metric for the *intra-TTI SINR variability* is defined as

$$\Delta\mathrm{SINR}[m] = \frac{\max\limits_{n\in[1,\dots3]}\{\mathrm{SINR_{slot}}[n]\}}{\min\limits_{n\in[1,\dots3]}\{\mathrm{SINR_{slot}}[n]\}} \quad . \qquad (3)$$

Further, to describe the SINR variation from the instant of CQI measurement at the UE to the time of downlink data transmission, the *link adaptation error* ($\varepsilon_{\mathrm{LA}}$) is defined as

$$\varepsilon_{\mathrm{LA}}[m] = \frac{\mathrm{SINR_{TTI}}[m+N_{delay}]}{\mathrm{SINR_{TTI}}[m]} \quad , \qquad (4)$$

where N_{delay} is the CQI feedback delay, assumed to be three as in [2]. Moreover, let the *HSDPA utilisation factor* (U) be defined as the average ratio of time the interfering sectors are transmitting power on the HS-DSCH. The remaining time no interfering HS-DSCH power is transmitted. Further, the fraction of total full load sector transmit power allocated to HS-DSCH transmission is denoted η. The remaining fraction of full load sector transmit power, i.e. $1-\eta$, used for e.g. pilot transmission, HSDPA control signalling, etc., is assumed time invariant. Moreover, the HS-DSCH of the serving sector is always on to maintain comparability of the throughput results. With these definitions, the partially loaded system has an *average other-sector interference level* ($I_{partial}$) given by

$$\begin{aligned} I_{partial} &= \eta\cdot U\cdot I_{full} + (1-\eta)\cdot I_{full} \\ &= (1-\eta\cdot(1-U))\cdot I_{full} \quad , \end{aligned} \qquad (5)$$

where I_{full} represents the average interference in a fully loaded system. If maximal possible cell throughput of the partially loaded system would be assessed with respect to a fully loaded system, one would encounter a cell throughput gain due to the reduced interference level. To focus on the effects of interference variability due to partial loading, the full load reference system is therefore operated with constant HS-DSCH transmit powers but with a generally reduced interference level in accordance with (5).

For a simple test case with non-dispersive *single input single output* (SISO) radio channels and only a single other-sector interferer, an upper bound of ΔSINR due to HS-DSCH on/off switching can be obtained as

$$\Delta SINR|_{single\_int} \leq \frac{1}{1-\eta} \quad . \qquad (6)$$

In a more representative situation where a user's received interference is coming from one dominant other-sector and all remaining sectors' interference powers can be combined in an equally strong but stable *additive white Gaussian noise* (AWGN) contribution, the upper bound becomes

$$\Delta SINR|_{\substack{single\_int\\+AWGN}} \leq \frac{1+(1-\eta\cdot(1-U))}{1-\eta+(1-\eta\cdot(1-U))} \quad , \qquad (7)$$

where $(1-\eta\cdot(1-U))$ relates to the AWGN contribution. Both cases are plotted in Fig. 2 as a function of η for a utilisation of $U=0.5$. The results indicate a significant potential variability for systems with large power fractions allocated to HSDPA. When using CLM1 worse upper bound SINR variations are expected even in a fully loaded system, simply caused by HS-DSCH transmit weight updates, i.e. due to possible switching from destructive to constructive interference signal additions including array gain.

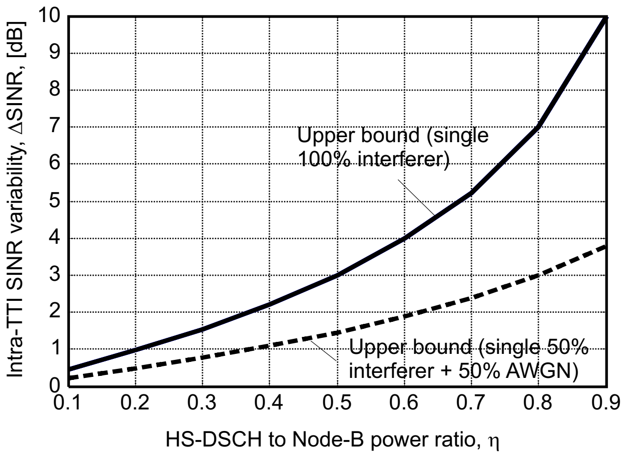

Figure 2. Upper bound SINR variations versus HS-DSCH sector power allocation under partial HSDPA activity (U=0.5).

III. System Model and Parameter Settings

Since variability is caused by many mechanisms and is highly dependent on the power loss between the UE and the interfering sectors, link, and quasi-static system simulations have been employed as depicted in Fig. 3. The effects of other-sector interference variation are studied for the hexagonal cell layout from [4, 5], where the centre cell is surrounded by two tiers of interfering cells. Each hexagonal cell is divided into three 120° sectors (see Fig. 1) amounting to a total of 57 sectors. In the SISO case, each sector deploys one directional transmit antenna element using the 3-sector antenna pattern from [4] with a 3 dB beamwidth of 70°. Two identical horizontally spaced elements are used in case of CLM1.

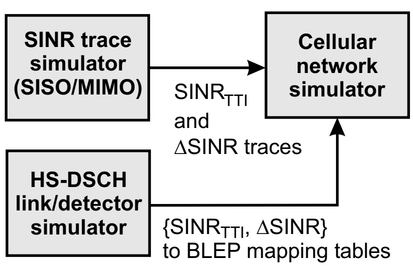

Figure 3. Simulation strategy overview.

The *SINR trace simulator* produces time evolving TTI-level SINR as well as ΔSINR traces. It uses an other-sector interference model that considers the interference from the two other sectors at the serving site, as well as the interference from the two strongest received sector powers from other sites accurately (see the black arrows in Fig. 1 that indicate the antenna pattern main lobes of the accurately modelled sectors as an example). The performance of this other-sector interference model is analysed in detail in [6] and is found to be sufficiently accurate to model the effect of other-sector interference variation. Although a real system might use slot or TTI synchronisation between sectors of the same site the interference model assumes the worst case situation of fully asynchronous switching instances between sectors. Hence, interference variations can occur any time within a TTI. The interference contribution from the remaining 52 sectors is modelled as constant AWGN. The interference model is based on every user's *line of sight angle of connection* (AoC) measured clockwise from the direction of the main lobe (Fig. 1) and on the *geometry factor* (G) defined as the ratio of own-sector small area mean, i.e. multipath fading averaged, received power to other-sector small area mean received power under full load [3]. The multipath fading channel characteristics of all 5 accurately modelled sectors are generated with the I-METRA MIMO channel model [7]. They follow the Vehicular A power delay profile and have Clarkes' type Doppler spectra. Similarly as in 'SCM Case II' [4], CLM1 transmit correlation is derived from a Laplacian power azimuth spectrum with root mean square angle spread of 2°/5°and element spacing of 10/0.5 wavelength for the *highly correlated* (hc) and the *weakly correlated* (wc) case respectively [8] [6]. As effects of other-sector interference variation gain in significance if the encountered own-sector interference is low an MMSE receiver is chosen to generate the necessary $\mathrm{SINR}_{\mathrm{TTI}}$ and ΔSINR traces. The rake receiver was found to exhibit more moderate variability results with similar trends.

The *HS-DSCH link/detector simulator* [9] includes the HS-DSCH turbo en- and decoder. It can estimate detector loss as a function of ΔSINR , where detector loss is defined as the required increase in $SINR_{TTI}$ to maintain a *block error probability* (BLEP) of 10%. It is further used to generate $\{\mathrm{SINR}_{\mathrm{TTI}}, \Delta\mathrm{SINR}\}$ to BLEP mapping tables for each modulation, coding, and multicode combination considered by the *link adaptation* (LA) algorithm. For this study, the original simulator [9] has been extended to include AoC-G based other-sector interference modelling [6].

The *cellular network simulator* with traffic modelling, LA, *incremental redundancy hybrid automatic repeat request* (IR H-ARQ), and PS capabilities [10, 11, 9], assigns an AoC-G value pair to every user based on a joint AoC-G probability density function [6]. G-factor and AoC remain constant during a user's session thus assuming that a packet call is short compared to the coherence time of the shadow fading and a user's movement in the angular domain. Based on the user's AoC-G value pair, the cellular network simulator determines a user's SINR performance through simple look-up of the appropriate $\mathrm{SINR}_{\mathrm{TTI}}$ and ΔSINR traces. To capture the effect of the employed modulation and coding schemes the $\{\mathrm{SINR}_{\mathrm{TTI}}, \Delta\mathrm{SINR}\}$ to BLEP mapping tables are used. Therewith the cellular network simulator is able to emulate every user's packet error performance and produce CQIs that in turn are used for link adaptation and packet scheduling. Due to an approximately 1 dB resolution of the applicable CQI feedback values, inaccuracy in the CQI reporting is inherent to the system. Another source of CQI inaccuracy are pilot channel estimation imperfections. To capture those effects system level performance results are either produced without CQI error or using a multiplicative log-normally distributed CQI error with a standard deviation of 1 dB, which, based on common UE performance requirements [12], seems to be a more realistic model. In both cases, the LA and PS delay of 3 TTI (6 ms) is considered. The simulator is configured to ensure that there are always 10 active users, thus creating a significant multiuser diversity order to be exploited by the PF PS. Whereas PF PS is used to study the joint impact of variability on link adaptation and CQI dependent scheduling, the FR PS is considered to study the isolated impact on link adaptation performance only. For detailed discussions of the scheduler settings and their optimisation see [11]. An overview of the parameter settings employed in the 3 subsimulators is given in Table 1.

Table 1
OVERALL PARAMETER SETTINGS.

Parameter	**Setting**
SINR trace simulator	
Cellular scenario	Macrocell [5]
Channel model	SCM Case II [4]
UE speed	3 km/h
Transmit correlation	wc, hc [6]
Receiver	MMSE
Channel/interference estimation	Ideal
CLM1 weight feedback	Error free & no delay
HS-DSCH-Node-B power ratio, η	70%
HSDPA other-sector utilisation, U	1.0, 0.5
HS-DSCH link/detector simulator	
Pilot-Node-B power ratio	10%
Channel estimation	Pilot-based, [10]
Oversampling	No
Cellular network simulator	
Number of multicodes	15
Number of users in serving sector	10
Traffic model	FIXD (800 kbit) [11]
LA/scheduling delay, N_{delay}	3 TTI
CQI error model	log-normal, 1.0 dB std
LA criterion	Max. 10% BLEP
Modulation	QPSK and 16QAM
Effective code rates	0.2-0.9 (step of 0.1)
IR H-ARQ model	See [9]
Packet scheduler	FR and PF
PF filter length,	250, [11]

IV. DISCUSSION OF RESULTS

Fig. 4a displays cell level $SINR_{TTI}$-statistics, where 'cell level' means that the statistics from all individual AoC-G dependent traces have been weighted and combined according to their AoC-G probabilities. It can be seen that there is only a marginal difference between the SINR statistics for full ($U = 1$) and partial ($U = 0.5$) utilisation. A zoom of the subplot would however reveal slightly increased variability in the partial case, i.e. there is only a marginally increased chance of high fading peaks as well as of deep fades. Generally, CLM1 achieves better SINR statistics than the SISO case as expected. Comparing the CLM1-wc against the CLM1-hc results it is found that the slope of the hc results is less steep, which can be attributed to less exploitable transmit diversity. However, the mean $SINR_{TTI}$ is 1.5 dB higher than for the wc case.

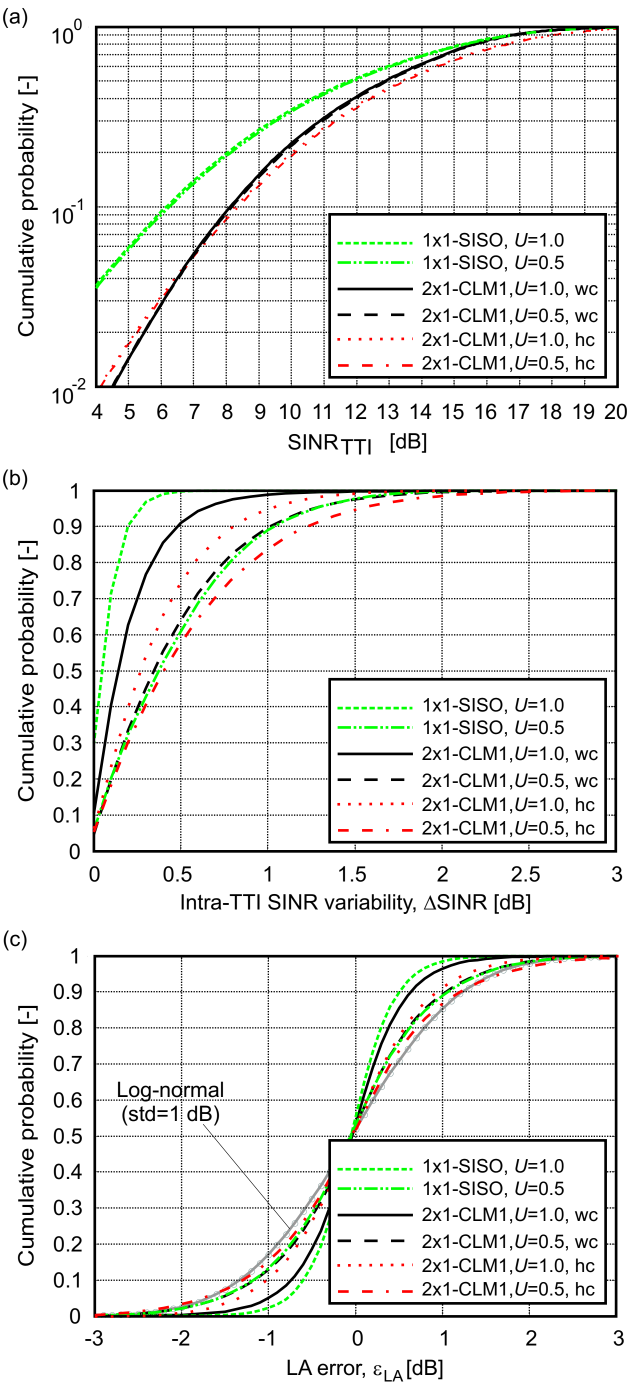

Figure 4. (a) TTI-level SINR statistics, (b) inter SINR variability, and (c) LA error statistics.

Fig. 4b displays the cell level ΔSINR *cumulative density function* (cdf) for the different transmission schemes. Doppler effects in the SISO case lead to a ΔSINR that for 90% of the cases is below 0.2 dB. Antenna weight switching can increase ΔSINR to around 0.5/0.8 dB at the 90% percentile for the wc/hc case respectively. The largest ΔSINR is obtained in case of partial HSDPA utilisation, reaching around 1 dB at the 90% percentile for the SISO as well as for the CLM1-wc case and around 1.25 dB for the CLM1-hc case. The generally higher ΔSINR of the hc case can be explained by the increased chance to encounter destructive as well as constructive interference signal combinations due to correlated channel transfer functions of similar magnitude. On the other hand the relative impact of on/off switching is smallest for the hc case that, due to weight updates alone, already experiences significant variability. Higher cell throughput losses are therefore expected for the SISO and CLM1-wc case when comparing full to partial HSDPA utilisation at system level.

A look at the cell level LA error statistics in Fig. 4c reveals that they follow exactly the same trends as their intra-TTI SINR variability counter parts. This is expected since Doppler effects are limited at the chosen UE speed and link adaptation delay. Additionally, Fig. 4c displays the variability used in the CQI error model, i.e. the cdf of a log-normal distributed variable with a standard deviation of 1 dB around zero mean. It can be seen that this log-normal distribution partly exceeds the variability caused by Doppler, partial HSDPA utilisation, and/or CLM1 weight switching. While the effects may be additive, this nevertheless suggests a limited impact of other-sector interference variations when CQI imperfections are considered.

A. *Effects of SINR Variability on Detector Performance*

In order to evaluate the detector loss versus ΔSINR the required SINR for a 10% BLEP has been extracted from link/detector simulations and is plotted in Fig. 5 for different modulation and coding settings. It can be seen that the turbo decoder of the HSDPA system experiences a significant degradation as ΔSINR increases, e.g. around 0.5 dB at 3 dB ΔSINR . Further, Fig. 5 shows that when ΔSINR is mainly caused by UE velocity and channel estimation imperfections ($U = 1.0$), the detector loss is about 0-0.25 dB smaller compared to the situation when it is caused by on/off HS-DSCH switching ($U = 0.5$). Some additional loss is expected since the abrupt SINR variations have an increased impact on the channel estimation algorithm which employs averaging. The additional loss of around 0.25 dB corresponds to only about 5-6% loss in user throughput when operating within the linear part of the HS-DSCH dynamic range. When seen in combination with the actual ΔSINR statistics from Fig. 4b, it is clear that this particular effect is minor when evaluated at system level. Hence, although relatively small but abrupt SINR changes are experienced during the TTI, the channel estimation and detection capabilities are robust enough not to yield large degradations of BLEP performance.

B. *Effects of SINR Variability on System Performance*

The results of the cellular network simulations with and without CQI measuring error (except for LA/PS delays which are still modelled) are listed in Table 2. The table shows the achieved cell throughput (carried load) for each transmission scheme, and packet scheduler. The Loss-column contains the loss in cell throughput when simulat-

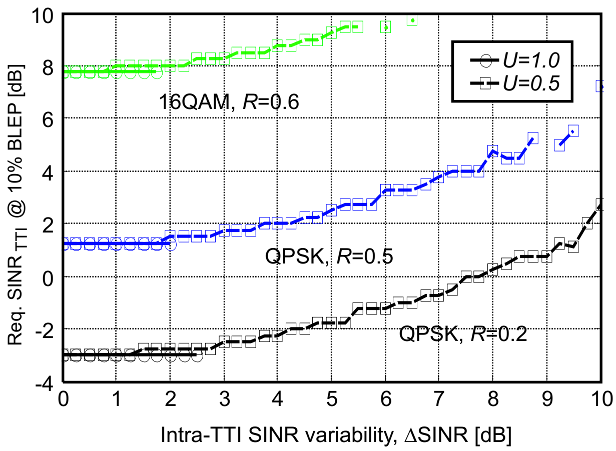

Figure 5. Detector loss versus intra-TTI SINR variability.

ing with $U = 0.5$ compared to $U = 1.0$. Generally, it should be noted that the results are repeatable within a margin of $\pm 2\%$ and simulation accuracy can only be improved though an extensive increase of simulation time.

As expected, if the CQI error model is used the effect of additional on/off switching is negligible and drowns in the simulation accuracy. For cases without CQI error, only the SISO and the CLM1-wc case suffer from additional on/off switching as already expected from the link level results. The fact that there is only a marginal difference in loss when comparing (SISO/CLM1-wc, CQI error off) FR PS against PF PS shows that the link adaptation unit suffers more from an increase in ε_{LA} than the PF scheduling unit. This can be explained by the fact that it is more likely to make a wrong link adaptation decision due to erroneous CQI feedback than to actually schedule the wrong user. Conversely this means that the PF PS algorithm at least for a relatively small number of users (i.e. 10) is quite robust to ε_{LA} triggered by on/off switching.

To answer the question if closed loop transmit diversity delivers a cell throughput gain compared to SISO when weight switching interference variation effects are considered one has to look at the absolute throughput numbers including CQI error. Dependent on the considered transmit correlation characteristics one can see that CLM1 combined with FR PS brings cell throughput gains in the order of 21 to 43%. These gains reduce to 11 to 33% for PF PS.

Table 2
SYSTEM LEVEL PERFORMANCE RESULTS.

Scheme	CQI error	Carr. load $U = 0.5$	Carr. load $U = 1.0$	Loss
FR PS				
1x1-SISO	Off	1.62 Mbps	1.70 Mbps	5%
2x1-CLM1, wc	Off	1.95 Mbps	2.07 Mbps	6%
2x1-CLM1, hc	Off	2.32 Mbps	2.28 Mbps	-2%
1x1-SISO	On	1.57 Mbps	1.57 Mbps	0%
2x1-CLM1, wc	On	1.92 Mbps	1.90 Mbps	-1%
2x1-CLM1, hc	On	2.24 Mbps	2.21 Mbps	-1%
PF PS				
1x1-SISO	Off	2.39 Mbps	2.67 Mbps	10%
2x1-CLM1, wc	Off	2.71 Mbps	2.86 Mbps	6%
2x1-CLM1, hc	Off	3.24 Mbps	3.20 Mbps	-1%
1x1-SISO	On	2.23 Mbps	2.18 Mbps	-2%
2x1-CLM1, wc	On	2.48 Mbps	2.48 Mbps	0%
2x1-CLM1, hc	On	2.96 Mbps	2.87 Mbps	-3%

V. Conclusions

The effects of other-sector interference variation due to partial HSDPA activity and closed loop transmit diversity operation have been evaluated. It was found that their impact on system level performance is negligible considering additionally a log-normal distributed CQI error with a 1 dB standard deviation. Much lower CQI error statistics will, however, be hard to achieve in practice due to limited CQI table resolution and practical measurement inaccuracies. Furthermore, CLM1 can maintain its cell throughput advantage over SISO despite negative influences from interfering sector weight updates. Hence, it is concluded that the WCDMA/HSDPA system is robust enough to handle the relatively small additional SINR fluctuations which would be introduced by partial HSDPA activity and/or closed loop transmit diversity operation.

VI. Acknowledgements

Many thanks to Laurent Schumacher and Troels Sørensen for their helpful comments.

References

[1] J. M. Holtzman, "Asymptotic Analysis of Proportional Fair Algorithm", in *12th IEEE International Symposium on Personal, Indoor and Mobile Radio Communications*, 2001, vol. 2, pp. F33–F37.

[2] J. Ramiro-Moreno, K. I. Pedersen, and P. E. Mogensen, "Network Performance of Transmit and Receive Diversity in HSDPA under Different Packet Scheduling Strategies", in *IEEE 57th Vehicular Technology Conference*, Jeju, Korea, April 2003, vol. 2, pp. 1454–1458.

[3] H. Holma and A. Toskala, Eds., *WCDMA for UMTS, Radio Access For Third Generation Mobile Communications*, Wiley, Chichester, UK, second edition, 2002.

[4] Spatial Channel Model Ad-Hoc Group, "Spatial Channel Model Text Description", Tech. Rep. SCM-134 v6.0, 3GPP/3GPP2, April 2003.

[5] 3GPP, "Feasibility Study for OFDM for UTRAN enhancement", Technical Specifications TR 25.892 (V0.1.1), Technical Specification Group Radio Access Network, Febuary 2003.

[6] L. T. Berger, T. E. Kolding, L. Schumacher, and P. E. Mogensen, "Geometry Based Other-Sector Interference Models for 3G Downlink System Simulations", in *The Seventh International Symposium on Wireless Personal Multimedia Communications (WPMC04)*, Abano Terme, Italy, September 2004, accepted for publication.

[7] J. P. Kermoal, L. Schumacher, K. I. Pedersen, P. E. Mogensen, and F. Frederiksen, "A Stochastic MIMO Radio Channel Model with Experimental Validation", *IEEE Journal on Selected Areas in Communications*, vol. 20, no. 6, pp. 1211–1226, August 2002.

[8] L. Schumacher, K. I. Pedersen, and P. E. Mogensen, "From Antenna Spacing to Theoretical Capacities - Guidelines for Simulating MIMO Systems", in *PIMRC*, 2002, pp. 587–592.

[9] F. Frederiksen and T. E. Kolding, "Performance and Modeling of WCDMA/HSDPA Transmission/H-ARQ Schemes", in *IEEE 56th Vehicular Technology Conference*, Vancouver, Canada, September 2002, vol. 1, pp. 472–476.

[10] T. E. Kolding, F. Frederiksen, and P. E. Mogensen, "Performance Aspects of WCDMA Systems with High Speed Downlink Packet Access (HSDPA)", in *IEEE 56th Vehicular Technology Conference*, Vancouver, Canada, September 2002, vol. 1, pp. 477–481.

[11] T. E. Kolding, "Link and System Performance Aspects of Proportional Fair Scheduling in WCDMA/HSDPA", in *IEEE 58th Vehicular Technology Conference*, Orlando, USA, October 2003, vol. 3, pp. 1717–1722.

[12] 3GPP, "User Equipment (UE) radio transmission and reception (FDD)", Technical Specification TS 25.101 (V6.4.0), Technical Specification Group Radio Access Network, March 2004.